Clean transfer of graphene on Pt foils mediated by a carbon monoxide intercalation process

Article *in* Nano Research · June 2013

Impact Factor: 7.01 · DOI: 10.1007/s12274-013-0342-6

7 authors, including:

Y. F. Zhang
Peking University
107 PUBLICATIONS **2,274** CITATIONS
SEE PROFILE

Qingqing Ji
Peking University
38 PUBLICATIONS **485** CITATIONS
SEE PROFILE

Teng Gao
Peking University
43 PUBLICATIONS **842** CITATIONS
SEE PROFILE

Yu Zhang
Peking University
29 PUBLICATIONS **383** CITATIONS
SEE PROFILE

Nano Research 2013, 6(9): 671–678
DOI 10.1007/s12274-013-0342-6
Research Article

ISSN 1998-0124
CN 11-5974/O4

Clean transfer of graphene on Pt foils mediated by a carbon monoxide intercalation process

Donglin Ma[1], Yanfeng Zhang[1,2] (✉), Mengxi Liu[1], Qingqing Ji[1], Teng Gao[1], Yu Zhang[1,2], and Zhongfan Liu[1] (✉)

[1] *Center for Nanochemistry (CNC), Beijing National Laboratory for Molecular Sciences, College of Chemistry and Molecular Engineering, Academy for Advanced Interdisciplinary Studies, Peking University, Beijing 100871, China*
[2] *Department of Materials Science and Engineering, College of Engineering, Peking University, Beijing 100871, China*

Received: 19 March 2013
Revised: 10 June 2013
Accepted: 12 June 2013

KEYWORDS

graphene transfer,
clean,
etching free,
CO intercalation,
Pt foils

ABSTRACT

Noble metals such as Pt are a perfect substrate for the catalytic growth of monolayer graphene. However, the requirements of the subsequent transfer process are not compatible with the traditional etching method. In this work, we find that the interaction of graphene with Pt foil can be weakened through the intercalation of carbon monoxide (CO) under ambient pressure. This intercalation process occurs on both hexagonal-shape graphene islands and irregular graphene patches on changing the CO partial pressure from 0 to 0.6 MPa, as observed by scanning electron microscopy (SEM), Raman spectroscopy and X-ray photoemission spectroscopy. We demonstrate that, on a practical timescale, the intercalation ratio is proportional to the partial pressure of CO. Furthermore, we develop a clean transfer method of CO-intercalated graphene with water as a peeling agent. We show that this method enables the transfer of tens of micrometer-scale graphene patches onto SiO_2/Si, which are free from metal or oxide particle contamination. This transfer method should be a significant step towards the clean transfer of graphene, as well as the recyclable use of noble metal substrates.

1 Introduction

Graphene, a promising two dimensional (2D) material [1–3], exhibits various intriguing electronic properties such as high intrinsic carrier mobility [2] and linear dispersion of the Dirac electrons [4], which make it attractive for future applications in nanoelectronics [5] and optoelectronics [6]. For engineering such applications, batch production of high quality graphene is the first key issue. Chemical vapor deposition (CVD) has been proved to be the most suitable method, but because the growth is inevitably carried out on metal substrates like Cu [7, 8] or Ni [9, 10], a subsequent transfer process is necessary.

To date, the "PMMA-mediated" approach [7, 8, 10–13] is most commonly used for transferring graphene from metal substrates to arbitrary substrates. In this method, a layer of polymethylmethacrylate (PMMA)

Address correspondence to Yanfeng Zhang, yanfengzhang@pku.edu.cn; Zhongfan Liu, zfliu@pku.edu.cn

TSINGHUA UNIVERSITY PRESS Springer

is spin-coated onto graphene as a temporary support material, and then the metal substrate is etched away by oxidative etchants. The PMMA/graphene stack is then transferred onto arbitrary substrates. The PMMA is then removed by organic solvents to complete the transfer process. It is not so hard to imagine that the use of etching agents and supporting polymers usually introduces charged carriers and organic contaminants onto the transferred graphene. This was reported to dramatically reduce the carrier mobility of graphene on SiO_2 [14, 15]. Hence, developing a portable transfer method which introduces fewer impurities is considered to be the most significant step in developing practical applications of graphene.

Many different transfer methods have been proposed. Some of these have tried to reduce the amount of contaminants by using alternative etching agents such as ammonium persulfate [8, 16] or further surface cleaning [17, 18]. Other methods involve directly peeling off graphene by means of thermal release tapes [19, 20]. All these methods greatly reduce the amount of charged impurities on the transferred graphene. However, some organic contaminants from PMMA or thermal release tapes still remain on the graphene surfaces, which reduces the carrier mobility of the transferred graphene.

Recent research has found that a variety of metal or semi-metal atoms (Fe [21], Co [22], Au [23, 24], Mn [25], and Si [26–28]) and small molecules like O_2 [29], NO_2 [30], and H_2 [31] can intercalate into the space between graphene and single crystal substrates like Ru(0001) [27, 29], Rh(111) [21], SiC(0001) [25, 31] under ultrahigh vacuum (UHV) conditions. This intercalation process is considered to be a result of weak graphene–substrate interactions. Recently, CO intercalation into the interface of graphene/Pt(111) under UHV conditions has been thoroughly studied by Bao's group [32]. They showed that CO intercalation indeed occurred gradually under a certain CO pressure, and was initiated at substrate terraces and island edges.

Enlightened by this work, here we aim to explore the nature of CO intercalation into the interface of graphene on Pt foils due to the decoupling of graphene and Pt substrates under ambient pressure conditions, and characterize the resulting materials by scanning electron microscopy (SEM) and Raman spectroscopy. Ultimately, we hope the intercalation process can be utilized to develop a new transfer strategy, which in principle induces no charged particles or organic contaminants, thereby engineering a cleaner transfer technique.

2 Results and discussion

In parallel with the intensively explored system of graphene islands on Pt(111) under UHV conditions, CO molecules have been shown to be capable of intercalation into the interface of graphene islands on Pt foils. Furthermore, the intercalated structure of graphene/CO/Pt foils can be stable even after the CO supply was terminated [33], in contrast to the observed desorption of CO from graphene/CO/Pt(111) under UHV conditions. Figure 1(a) is a schematic illustration of the CO intercalation process. The interaction between graphene and Pt substrates is suggested to be weakened by the intercalation process.

In previous studies, we have successfully prepared monolayer or bilayer graphene on Pt foils via an atmospheric pressure chemical vapor deposition method (APCVD), and examined the continuity of graphene on the highly multifaceted textured substrates [34, 35]. In this work, graphene islands or patches were prepared in order to explore the intercalation process, because the plentiful edges in a sub-monolayer sample are more effective as intercalation fronts than a complete monolayer. In this case, a low pressure CVD method was utilized to prepare sub-monolayer graphene, and the typical SEM images are displayed in Figs. 1(b) and 1(f). Note that, increasing the pressure ratio of H_2 to CH_4 in the CVD growth process usually results in sharper boundaries or hexagonal-shape graphene islands (Fig. 1(b)).

In the intercalation process, the sample was placed in a gas cylinder which can supply CO partial pressure from 0 up to 0.6 MPa. For a better illustration of the experimental results, we selected a hexagonal-shape island as a candidate. It is intriguing to find that a contrast change from dark to gray at the island periphery is observed by SEM after exposing the sample to CO at 0.2 MPa (Fig. 1(c)) for 1 h. This contrast change may indicate the intercalation of CO, similar to the observed intercalation of CO into graphene on

Pt(111) [32]. The moderate reaction time is selected because by increasing the timescale from 1 h (even to as long as one day), the proportion of the intercalated region seemed almost unchanged. That suggests 1 h may be the saturation time for intercalation under atmospheric conditions.

When the partial pressure of CO was raised stepwise to 0.2, 0.4, and 0.6 MPa over 1 h, the intercalated area ratio increased towards the full intercalation of CO—from 37%, to 60%, and 100%, respectively. The edges of graphene islands seem to be the fronts triggering the CO intercalation, since the intercalated regions seen as gray contrasts extend from the edge to the inner part of the islands as shown by SEM (Figs. 1(c)–1(e)). Note that, when the partial pressure of CO reaches 0.6 MPa, the whole island becomes gray, and the contrast difference between the graphene islands and the SiO_2 substrate was minimized, probably indicating that the graphene island was fully intercalated by CO molecules (Atomic force microscope (AFM) images of graphene on Pt foils before and after CO intercalation are shown in Fig. S1 in the Electronic Supplementary Material (ESM)). Figure 1(j) exhibits statistical data of the coverage of the CO-intercalated area, which increase nearly monotonically with increasing CO partial pressure.

As supplementary samples, the interaction with CO of graphene islands having irregular boundaries is also displayed in Figs. 1(f)–1(i), which also show strong CO pressure dependence of the intercalated regions.

We further confirmed the intercalated nature of the material by spectroscopic methods. Raman spectroscopy measurements were performed to explore the different interactions between the intercalated and the normal graphene regions with the Pt substrate. Figure 2(a) is a large-area SEM image of a square-shape graphene island (the darker area in the center of the square graphene flake is multilayer graphene), which was partly intercalated by CO with the periphery of the island showing a gray contrast with regard to the inner part. A zoom-in image of the area marked with a red square in Fig. 2(b) presents more details of the SEM contrast difference. It is worthy of note that, the Pt grain boundary, spanning underneath the graphene flake (showing a weaker line contrast by SEM than that of the intercalated regions at the island periphery), may not act as the front for CO intercalation. In fact, a graphene wrinkle, seen as a darker line shape

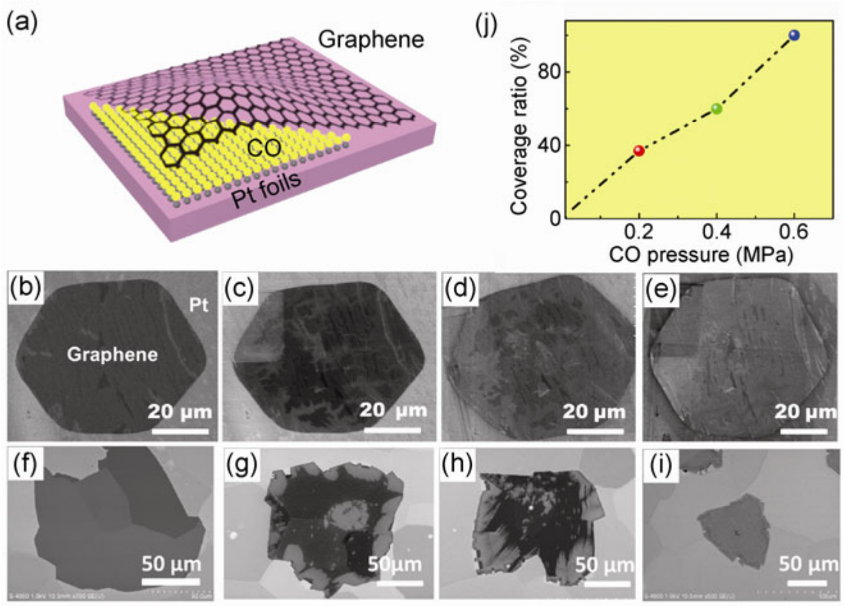

Figure 1 (a) Schematic illustration of CO intercalation into the interface of graphene on Pt foils. (b) SEM image of a hexagonal single-layer graphene on a polycrystalline Pt foil, which was grown with 8 standard cubic centimeters per minute (sccm) CH_4 and 700 sccm H_2 at 990 °C for 1 h. (c)–(e) Series of SEM images of the same graphene island in (b) after exposure to 0.2, 0.4, and 0.6 MPa CO at room temperature for 1 h, respectively. Lighter contrast on a graphene island is presumed to be the area intercalated by CO. (f)–(i) CO intercalation in the irregular shape graphene islands prepared with 10 sccm CH_4 and 700 sccm H_2 at 990 °C for 1 h. (j) Statistical diagram of CO intercalation ratio on graphene as function of CO partial pressure.

contrast on the graphene island surface, is where minor CO intercalation probably occurs with the appearance of some semicircular gray regions. That means, in addition to the island boundary, the graphene wrinkle may serve as another initial place for CO intercalation.

Figure 2(d) shows Raman spectra of pristine graphene on Pt foils (the orange circle in Fig. 2(b)) and the CO-intercalated area (purple dot in Fig. 2(b)). Similar to previous work [34], the intensity of the Raman 2D band (2,650–2,750 cm^{-1}) on native graphene is greatly weakened and the G band is shifted to 1,600 cm^{-1} due to the substrate effect (more Raman data are shown in Fig. S2 in the ESM). Surprisingly, in the intercalated region, the 2D band presents a typical single Lorentzian shape at 2,677 cm^{-1}, with a full width at half-maximum (FWHM) of 31 cm^{-1} and an intensity ratio of 2D band to G band (I_{2D}/I_G) in the range of 2–3. This spectral feature is comparable to monolayer graphene on SiO_2/Si, thus providing solid evidence of the greatly weakened interaction between graphene and the Pt substrate. Hence, Raman spectra of monolayer graphene can be obtained with a high fidelity. Note that, on the hexagonal-shape graphene island with partial CO intercalation (Fig. 2(c)), the differences in Raman spectra between the native and the intercalated regions also show the same features as in Fig. 2(d).

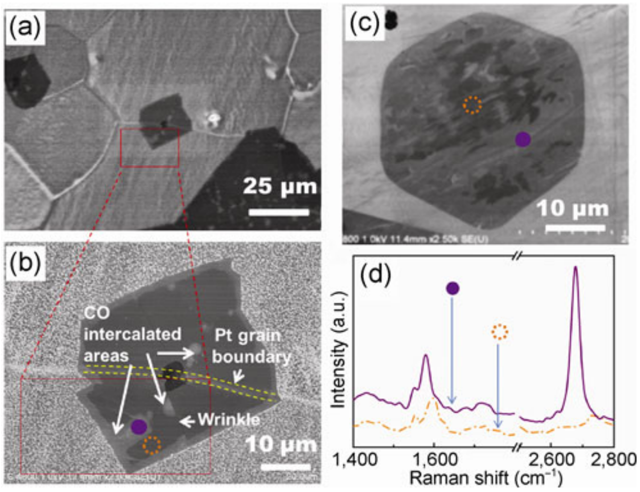

Figure 2 (a) Large-area SEM image of sub-monolayer graphene on Pt foils. (b) Zoom-in image of the square-shape graphene flake in (a). Lighter contrast on the graphene flake corresponds to the CO-intercalated area. (c) SEM image showing partial CO intercalation on a hexagonal-shape graphene island. (d) The upper and lower spectra in Fig. 2(d) are recorded from the regions indicated with purple spots or orange circles, referring to CO-intercalated and native graphene areas in (b), respectively.

We also performed X-ray photoelectron spectroscopy (XPS) measurements to confirm the CO intercalation behavior. Figures 3(a) and 3(b) are SEM images of a mostly CO-intercalated graphene on Pt foils. The coverage of graphene on the Pt foils is ~0.6 monolayer. Figure 3(c) shows survey spectra of the sample in Figs. 3(a) and 3(b). In addition to the typical peaks of Pt substrates, C 1s and O 1s peaks are also visible in the spectra. The signal of C 1s at 284.8 eV can be mainly attributed to graphene, as reported for exfoliated graphene [36]. The O 1s signal can be attributed to intercalated CO molecules. Fine details of the O 1s spectra are exhibited in Fig. 3(d): There are two peaks at 532.4 and 530.6 eV corresponding to CO adsorption at the top site and bridge site of Pt(111), respectively [37]. This evidence further proves that CO molecules are indeed located below graphene.

The above experimental results confirm that CO intercalation into the interface of graphene on Pt foils can dramatically decrease the coupling between the overlayer and the substrate. This suggests that this intercalation process can be effective in developing new graphene transfer method, which does not require etching the metal substrate. We selected two methods to transfer the graphene. As schematically shown in Fig. 4, graphene was initially synthesized on Pt foils,

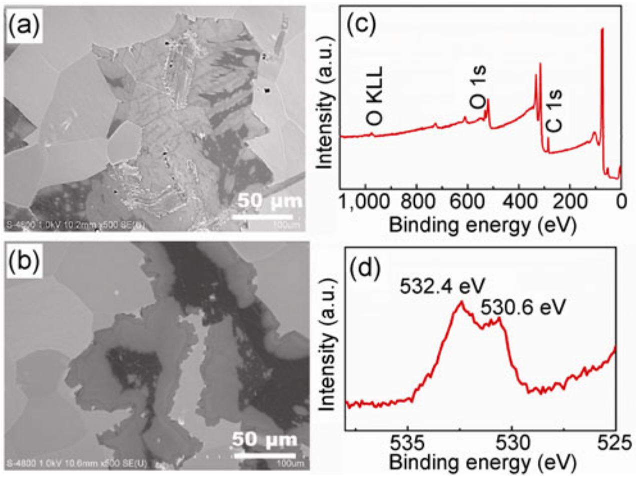

Figure 3 (a) and (b) SEM images of CO-intercalated graphene on Pt foils prepared for XPS analysis. (c) and (d) XPS survey spectra and O 1s spectra of the samples in (a) and (b), respectively.

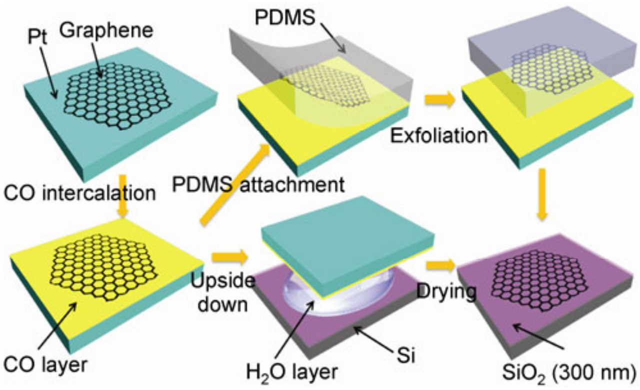

Figure 4 Synthesis, intercalation, and transfer process for CO-intercalated graphene onto SiO_2/Si.

and then CO was intercalated into the interface of graphene and Pt under ambient pressure with a CO pressure of 0.6 MPa, resulting in a CO layer underneath. Afterwards, two distinct transfer processes were designed. A solid poly(dimethylsiloxane) (PDMS) stamp was directly attached to the CO-intercalated graphene to adsorb the graphene layer, by using the moderate adhesion force between solid PDMS and graphene. The PDMS stamp was then pressed down on a SiO_2/Si substrate, leading to adsorption of graphene on SiO_2/Si. Unlike the conventional method, this transfer process does not require etching of the metal substrate, or the removal of a soft supporting material. Thus, problems associated with the presence of inorganic ions such as Fe^{3+} introduced by the etching process and organic residues such as PMMA, which usually serve as extraneous scattering centers and suppress the carrier mobility of intrinsic graphene, are eliminated in our nearly clean transfer method.

An alternative transfer method involves peeling off the CO-intercalated graphene from Pt foils with water being a special stamp. As shown in Fig. 4, the CO-intercalated graphene on Pt foil was turned upside down and pressed onto plasma-treated SiO_2/Si, with the substrate decorated by a drop of deionized water. The reason for plasma treatment of SiO_2 prior to graphene transfer is to improve the hydrophilicity of SiO_2/Si, so that water can form a uniform water membrane on the surface. After the graphene layer was pressed on SiO_2, a nearly homogenous soaking of water into graphene can be realized, resulting in a uniform surface tension on the water surface. This surface tension can serve as a driving force for the exfoliation of graphene. As a result, graphene was peeled off from the Pt foil and became attached to the SiO_2/Si substrate. Note that different from previous transfer processes, where a soft support material such as PMMA, PDMS or thermal release tape was employed, the water-assisted transfer method is totally free from soft support materials resulting the complete absence of organic residues.

To characterize the quality of the transferred graphene, we then performed Raman spectroscopy on both samples. As shown in the optical image in Fig. 5(a), tens of micron-sized graphene flakes have been transferred onto SiO_2/Si substrates using the first method. The size of the flake can be varied from several microns to tens of microns, limited by the current unoptimized transfer conditions (more OM data are presented in Fig. S3 in the ESM). Figure 5(b) shows a Raman spectrum collected randomly on the transferred graphene flakes with the laser spot away from the folded regions on the flake boundary. It shows a G band located at 1,582 cm^{-1} and a 2D band at 2,682 cm^{-1} with a narrow FWHM of ~30 cm^{-1}, along with a I_{2D}/I_G ratio in the range of 2–3. No obvious D band can be observed around 1,350 cm^{-1}. These results confirm the monolayer nature, as well as the high crystal quality, of the transferred graphene.

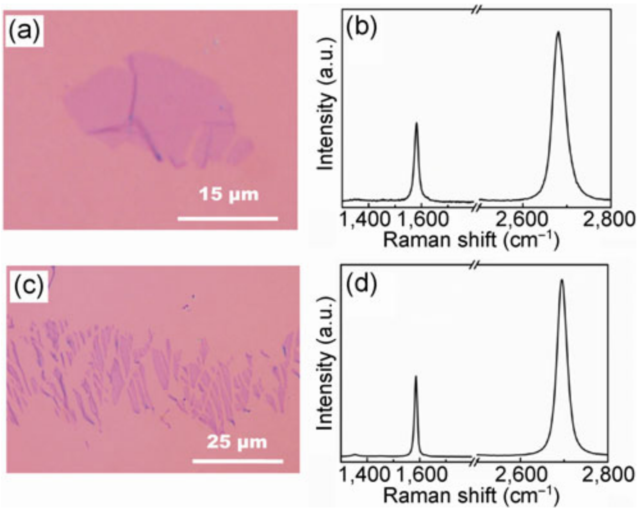

Figure 5 (a) and (c) Optical images of CO-intercalated graphene on Pt foils after being transferred onto SiO_2/Si by PDMS and H_2O, respectively. (b) and (d) The corresponding Raman spectra of the samples transferred onto SiO_2/Si.

With the second transfer method, we find that many graphene flakes appear on SiO_2/Si substrates, showing purple-like contrast with regard to the SiO_2 substrate by optical microscopy (Fig. 5(c)). Compared to the first transfer method, graphene flakes transferred using this strategy are a little smaller in size (more comparative OM images are shown in Fig. S4 in the ESM). We suggest that this is due to the overstress of water surface tension on the intralayer mechanical strength of monolayer graphene. In this case, finding a suitable liquid with lower surface tension may improve the continuity of the transferred graphene to some extent. As shown in Fig. 5(d), graphene transferred by this method also exhibits good film quality, since there is only a very weak D band in the Raman spectra. Note that, compared with the material obtained using the first transfer method, the 2D band, with a narrow FWHM of ~30 cm^{-1}, is slightly red-shifted from 2,682 to 2,695 cm^{-1}. This shift in 2D peak to higher wavelength by ~13 cm^{-1} can be understood in terms of a high p-doping effect due to the involvement of water in the transfer process. We believe that after appropriate annealing of the sample obtained by water-assisted transfer, this doping effect may be weakened to some extent.

3 Conclusion

We have explored the CO intercalation process for graphene on Pt foils under ambient pressure conditions. Evidence from SEM images and Raman spectra proves that CO intercalation is significantly dependent on the partial pressure of CO. The difference between this system and the intercalation of CO into graphene on Pt(111) in a UHV system is that CO molecules can be confined in the space between graphene and Pt foil after the CO atmosphere is removed and the sample removed from the reaction chamber. The CO intercalation process under ambient pressure was exploited as a basis for developing a novel transfer strategy. Two specific transfer processes were found to be effective in the successful transfer of sub-monolayer graphene onto SiO_2/Si substrates. We believe that this work provides a new way of optimizing graphene transfer, especially for graphene grown on noble metal substrates.

Acknowledgements

This work was financially supported by the Ministry of Science and Technology of China (Grant Nos. 2011CB921903, 2012CB921404, 2012CB933404, 2013CB932603, and 2011CB933003), and the National Natural Science Foundation of China (Grant Nos. 21073003, 51222201, 51290272, 51121091, and 51072004).

Electronic Supplementary Material: Supplementary material (further details of the SEM measurements, AFM imaging, and Raman spectroscopy measurements) is available in the online version of this article at http://dx.doi.org/10.1007/s12274-013-0342-6.

References

[1] Geim, A. K.; Novoselov, K. S. The rise of graphene. *Nat. Mater*. **2007**, *6*, 183–191.

[2] Novoselov, K. S.; Geim, A. K.; Morozov, S. V.; Jiang, D.; Zhang, Y.; Dubonos, S. V.; Grigorieva, I. V.; Firsov, A. A. Electric field effect in atomically thin carbon films. *Science* **2004**, *306*, 666–669.

[3] Novoselov, K. S.; Geim, A. K.; Morozov, S. V.; Jiang, D.; Katsnelson, M. I.; Grigorieva, I. V.; Dubonos, S. V.; Firsov, A. A. Two-dimensional gas of massless Dirac fermions in graphene. *Nature* **2005**, *438*, 197–200.

[4] Nair, R. R.; Blake, P.; Grigorenko, A. N.; Novoselov, K. S.; Booth, T. J.; Stauber, T.; Peres, N. M. R.; Geim, A. K. Fine structure constant defines visual transparency of graphene. *Science* **2008**, *320*, 1308.

[5] Schwierz, F. Graphene transistors. *Nat. Nanotechnol*. **2010**, *5*, 487–496.

[6] Bonaccorso, F.; Sun, Z.; Hasan, T.; Ferrari, A. C. Graphene photonics and optoelectronics. *Nat. Photons* **2010**, *4*, 611–622.

[7] Li, X.; Cai, W.; An, J.; Kim, S.; Nah, J.; Yang, D.; Piner, R.; Velamakanni, A.; Jung, I.; Tutuc, E. et al. Large-area synthesis of high-quality and uniform graphene films on copper foils. *Science* **2009**, *324*, 1312–1314.

[8] Bae, S.; Kim, H.; Lee, Y.; Xu, X.; Park, J. S.; Zheng, Y.; Balakrishnan, J.; Lei, T.; Ri Kim, H.; Song, Y. I. et al. Roll-to-roll production of 30-inch graphene films for transparent electrodes. *Nat. Nanotechnol*. **2010**, *5*, 574–578.

[9] Kim, K. S.; Zhao, Y.; Jang, H.; Lee, S. Y.; Kim, J. M.; Kim, K. S.; Ahn, J. H.; Kim, P.; Choi, J. Y.; Hong, B. H. Large-scale pattern growth of graphene films for stretchable transparent electrodes. *Nature* **2009**, *457*, 706–710.

[10] Reina, A.; Jia, X.; Ho, J.; Nezich, D.; Son, H.; Bulovic, V.; Dresselhaus, M. S.; Kong, J. Large area, few-layer graphene films on arbitrary substrates by chemical vapor deposition. *Nano Lett*. **2009**, *9*, 30–35.

[11] Li, X.; Zhu, Y.; Cai, W.; Borysiak, M.; Han, B.; Chen, D.; Piner, R. D.; Colombo, L.; Ruoff, R. S. Transfer of large-area graphene films for high-performance transparent conductive electrodes. *Nano Lett*. **2009**, *9*, 4359–4363.

[12] Yan, Z.; Lin, J.; Peng, Z.; Sun, Z.; Zhu, Y.; Li, L.; Xiang, C.; Samuel, E. L.; Kittrell, C.; Tour, J. M. Toward the synthesis of wafer-scale single-crystal graphene on copper foils. *ACS Nano* **2012**, *6*, 9110–9117.

[13] Liu, N.; Fu, L.; Dai, B.; Yan, K.; Liu, X.; Zhao, R.; Zhang, Y.; Liu, Z. Universal segregation growth approach to wafer-size graphene from non-noble metals. *Nano Lett*. **2011**, *11*, 297–303.

[14] Chen, J. H.; Jang, C.; Adam, S.; Fuhrer, M. S.; Williams, E. D.; Ishigami, M. Charged-impurity scattering in graphene. *Nat. Phys*. **2008**, *4*, 377–381.

[15] Chen, J. H.; Jang, C.; Xiao, S.; Ishigami, M.; Fuhrer, M. S. Intrinsic and extrinsic performance limits of graphene devices on SiO_2. *Nat. Nanotechnol*. **2008**, *3*, 206–209.

[16] Suk, J. W.; Kitt, A.; Magnuson, C. W.; Hao, Y.; Ahmed, S.; An, J.; Swan, A. K.; Goldberg, B. B.; Ruoff, R. S. Transfer of CVD-grown monolayer graphene onto arbitrary substrates. *ACS Nano* **2011**, *5*, 6916–6924.

[17] Liang, X.; Sperling, B. A.; Calizo, I.; Cheng, G.; Hacker, C. A.; Zhang, Q.; Obeng, Y.; Yan, K.; Peng, H.; Li, Q. et al. Toward clean and crackless transfer of graphene. *ACS Nano* **2011**, *5*, 9144–9153.

[18] Shin, D. W.; Lee, H. M.; Yu, S. M.; Lim, K. S.; Jung, J. H.; Kim, M. K.; Kim, S. W.; Han, J. H.; Ruoff, R. S.; Yoo, J. B. A facile route to recover intrinsic graphene over large scale. *ACS Nano* **2012**, *6*, 7781–7788.

[19] Caldwell, J. D.; Anderson, T. J.; Culbertson, J. C.; Jernigan, G. G.; Hobart, K. D.; Kub, F. J.; Tadjer, M. J.; Tedesco, J. L.; Hite, J. K.; Mastro, M. A. et al. Technique for the dry transfer of epitaxial graphene onto arbitrary substrates. *ACS Nano* **2010**, *4*, 1108–1114.

[20] Charlotte, H.; Markus, K.; Nedjma, B.; Stefan, S.; Daniel, F. F.; Johann, C.; Klaus, M.; Thomas, M.; Carsten, B. Mechanical exfoliation of epitaxial graphene on Ir(111) enabled by Br_2 intercalation. *J. Phys: Condens. Matter* **2012**, *24*, 314208.

[21] Sicot, M.; Leicht, P.; Zusan, A.; Bouvron, S.; Zander, O.; Weser, M.; Dedkov, Y. S.; Horn, K.; Fonin, M. Size-selected epitaxial nanoislands underneath graphene moiré on Rh(111). *ACS Nano* **2012**, *6*, 151–158.

[22] Decker, R.; Brede, J.; Atodiresei, N.; Caciuc, V.; Blügel, S.; Wiesendanger, R. Atomic-scale magnetism of cobalt-intercalated graphene. *Phys. Rev. B* **2013**, *87*, 041403.

[23] Gierz, I.; Suzuki, T.; Weitz, R. T.; Lee, D. S.; Krauss, B.; Riedl, C.; Starke, U.; Höchst, H.; Smet, J. H.; Ast, C. R. et al. Electronic decoupling of an epitaxial graphene monolayer by gold intercalation. *Phys. Rev. B* **2010**, *81*, 235408.

[24] Varykhalov, A.; Sánchez-Barriga, J.; Shikin, A. M.; Biswas, C.; Vescovo, E.; Rybkin, A.; Marchenko, D.; Rader, O. Electronic and magnetic properties of quasifreestanding graphene on Ni. *Phys. Rev. Lett*. **2008**, *101*, 157601.

[25] Gao, T.; Gao, Y.; Chang, C.; Chen, Y.; Liu, M.; Xie, S.; He, K.; Ma, X.; Zhang, Y.; Liu, Z. Atomic-scale morphology and electronic structure of manganese atomic layers underneath epitaxial graphene on SiC(0001). *ACS Nano* **2012**, *6*, 6562–6568.

[26] Lizzit, S.; Larciprete, R.; Lacovig, P.; Dalmiglio, M.; Orlando, F.; Baraldi, A.; Gammelgaard, L.; Barreto, L.; Bianchi, M.; Perkins, E. et al. Transfer-free electrical insulation of epitaxial graphene from its metal substrate. *Nano Lett*. **2012**, *12*, 4503–4507.

[27] Mao, J.; Huang, L.; Pan, Y.; Gao, M.; He, J.; Zhou, H.; Guo, H.; Tian, Y.; Zou, Q.; Zhang, L. et al. Silicon layer intercalation of centimeter-scale, epitaxially grown monolayer graphene on Ru(0001). *Appl. Phys. Lett*. **2012**, *100*, 093101.

[28] Cui, Y.; Gao, J.; Jin, L.; Zhao, J.; Tan, D.; Fu, Q.; Bao, X. An exchange intercalation mechanism for the formation of a two-dimensional Si structure underneath graphene. *Nano Res*. **2012**, *5*, 352–360.

[29] Zhang, H.; Fu, Q.; Cui, Y.; Tan, D.; Bao, X. Growth mechanism of graphene on Ru(0001) and O_2 adsorption on the graphene/Ru(0001) surface. *J. Phys. Chem. C* **2009**, *113*, 8296–8301.

[30] Sutter, P.; Sadowski, J. T.; Sutter, E. A. Chemistry under cover: Tuning metal−graphene interaction by reactive intercalation. *J. Am. Chem. Soc*. **2010**, *132*, 8175–8179.

[31] Riedl, C.; Coletti, C.; Iwasaki, T.; Zakharov, A. A.; Starke, U. Quasi-free-standing epitaxial graphene on SiC obtained by hydrogen intercalation. *Phys. Rev. Lett*. **2009**, *103*, 246804.

[32] Mu, R.; Fu, Q.; Jin, L.; Yu, L.; Fang, G.; Tan, D.; Bao, X. Visualizing chemical reactions confined under graphene. *Angew. Chem. Int. Ed*. **2012**, *51*, 4856–4859.

[33] Gland, J. L.; Kollin, E. B. Carbon monoxide oxidation on the Pt(111) surface: Temperature programmed reaction of coadsorbed atomic oxygen and carbon monoxide. *J. Chem. Phys*. **1983**, *78*, 963–974.

[34] Gao, T.; Xie, S.; Gao, Y.; Liu, M.; Chen, Y.; Zhang, Y.; Liu, Z. Growth and atomic-scale characterizations of graphene on multifaceted textured Pt foils prepared by chemical vapor deposition. *ACS Nano* **2011**, *5*, 9194–9201.

[35] Gao, L.; Ren, W.; Xu, H.; Jin, L.; Wang, Z.; Ma, T.; Ma, L. P.; Zhang, Z.; Fu, Q.; Peng, L. M.; et al. Repeated growth and bubbling transfer of graphene with millimetre-size single-crystal grains using platinum. *Nat. Commun*. **2012**, *3*, 699.

[36] Zheng, J.; Liu, H. T.; Wu, B.; Di, C. A.; Guo, Y. L.; Wu, T.; Yu, G.; Liu, Y. Q.; Zhu, D. B. Production of graphite chloride and bromide using microwave sparks. *Sci. Rep.* **2012**, *2*, 662.

[37] Kinne, M.; Fuhrmann, T.; Zhu, J. F.; Tränkenschuh, B.; Denecke, R.; Steinrück, H. P. Coadsorption of D_2O and CO on Pt(111) studied by *in situ* high-resolution X-ray photoelectron spectroscopy. *Langmuir* **2004**, *20*, 1819–1826.